Electronic Supplementary Material (ESI) for Physical Chemistry Chemical Physics.

Supplementary Information

Characterizing allosteric inhibitor-induced inactive state in With-No-Lysine kinase 1 using Gaussian accelerated molecular dynamic simulations

Nisha Amarnath Jonniya, Md Fulbabu Sk, Parimal Kar*

Department of Biosciences and Biomedical Engineering, Indian Institute of Technology Indore, Khandwa Road, MP 453552, India.

*Corresponding author: Parimal Kar | Email: parimal@iiti.ac.in

Table S1. Per-residue contributions to binding free energy calculated using the MM/GBSA scheme.

Residue	T_{vdW}	T_{ele}	T_{GB}	T_{np}	T_S	T_B	T_{TOT}
WNK1/CI							
Phe283	-2.3	-0.1	0.2	-0.2	-2.3	-0.1	-2.4
Met304	-1.5	-2.2	1.6	-0.1	-1.2	-1.0	-2.2
Val235	-1.9	-0.1	0.1	-0.2	-1.9	-0.2	-2.1
Phe356	-2.4	-0.5	1.1	-0.3	-2.1	-0.1	-2.1
Val281	-1.4	0.3	-0.3	-0.1	-1.2	-0.3	-1.5
Leu303	-0.7	-1.2	0.5	0.0	-0.4	-1.0	-1.4
Leu369	-2.0	-1.1	1.9	-0.2	-1.0	-0.4	-1.4
Thr301	-1.7	-0.4	1.0	-0.2	-1.1	-0.3	-1.3
Leu299	-1.2	0.0	0.1	-0.1	-1.2	-0.1	-1.2
Gly367	-0.9	-0.3	0.1	0.0	-0.3	-0.9	-1.2
Lys233	-0.8	-2.0	1.8	-0.1	-1.1	0.0	-1.2
Leu371	-1.1	0.2	-0.1	-0.1	-1.0	-0.1	-1.2
WNK1/AI							
Leu369	-3.9	-0.6	1.5	-0.3	-2.6	-0.7	-3.3
Arg255	-0.9	-9.6	7.7	-0.2	-3.1	0.0	-3.1
Leu272	-2.8	-0.5	0.8	-0.3	-2.6	-0.3	-2.9
Leu299	-2.0	0.0	0.1	-0.2	-1.9	-0.2	-2.1
Phe283	-2.3	-0.3	0.9	-0.1	-1.5	-0.4	-1.9
Val281	-0.6	-3.0	2.0	-0.1	-0.6	-1.1	-1.7
Ile297	-1.0	-0.2	0.2	-0.1	-1.0	-0.1	-1.2

Table S2. Computational Alanine-Scanning (CAS) mutagenesis binding components between WNK1-AI inhibitors. The binding energy is given in kcal/mol, and the standard error of the mean is provided in parentheses.

System	ΔE_{vdW}	ΔE_{elec}	ΔG_{pol}	ΔG_{np}	ΔG_{bind}	$\Delta\Delta G_{bind}^{a}$
WT	-61.78 (0.03)	-31.10 (0.04)	57.22 (0.04)	-5.44 (0.0)	-41.11 (0.03)	
L369A	-59.26 (0.03)	-30.81 (0.04)	55.91 (0.04)	-5.55 (0.0)	-39.71 (0.03)	1.4 (0.03)
R255A	-60.26 (0.02)	-11.95 (0.03)	41.95 (0.04)	-5.37 (0.0)	-35.64 (0.03)	5.47 (0.03)
L272A	-57.69 (0.02)	-30.93 (0.04)	56.25 (0.04)	-5.53 (0.0)	-37.90 (0.03)	3.21 (0.03)
I297A	-60.22 (0.03)	-31.0 (0.04)	57.04 (0.04)	-5.50 (0.0)	-39.68 (0.03)	1.43 (0.03)
E268A	-60.39 (0.02)	-24.70 (0.04)	49.99 (0.03)	-5.46 (0.0)	-40.56 (0.03)	0.55 (0.03)
V281A	-61.29 (0.03)	-31.09 (0.04)	57.21 (0.04)	-5.46 (0.0)	-40.63 (0.03)	0.48 (0.03)

$\Delta\Delta G_{bind}^{a} = \Delta G_{bind}^{mut} - \Delta G_{bind}^{WT}$

Table S3. Hydrogen bond interactions calculated in the simulations between WNK1 and inhibitors, such as competitive and allosteric inhibitors.

Systems	Acceptor	Donor	Distance (Å)	Angle (º)	Occupancy (%)[a]
WNK1-CI	CI@N37	M304@N	2.92	159.36	30.41
	CI@O42	K233@NZ(HZ1)	2.82	157.73	18.23
	CI@O42	K233@NZ(HZ3)	2.82	157.65	17.41
	CI@O42	K233@NZ(HZ2)	2.82	157.66	17.15
	CI@H312	D368@NH	2.86	147.65	7.86
	CI@N13	D368@NH	2.92	147.19	5.78
WNK1-AI	V281@O	AI@NH23	2.84	161.71	81.72
	AI@O11	R255@NE	2.84	155.07	41.74
	AI@O11	R255@NH2	2.87	146.78	16.23
	AI@O25	R255@NH2	2.89	144.46	7.30

A hydrogen bond is defined by an acceptor-donor atom distance of ≤ 3.5Å and acceptor-H-donor angle of ≥120º.

[a]Occupancy is the percentage of hydrogen bond during the simulation time.

Table S4. WNK1-Inhibitors non-bonded interactions of the last trajectory from the GaMD simulations calculated from the Discovery Studio. [a]donor hydrogen acceptor.

Name	Distance	Angle DHA[a]	Category	Type of Interactions
WNK1-CI				
K233@HZ1-CI@O42	1.82	160.78	Hydrogen-bond	Conventional-H-bond
M304@HN-CI@N37	2.00	176.03	Hydrogen-bond	Conventional-H-bond
A269@HA-CI@F4	2.30	156.89	Hydrogen-bond	Carbon-H-bond
L303@HA-CI@N37	2.83	146.49	Hydrogen-bond	Carbon-H-bond
CI@H11-V281@O	2.57	167.20	Hydrogen-bond	Carbon-H-bond
CI@H202-D368@OD2	2.24	142.21	Hydrogen-bond	Carbon-H-bond
CI@H312-D368@OD2	2.93	127.36	Hydrogen-bond	Carbon-H-bond
CI@H35-E302@O	2.52	145.32	Hydrogen-bond	Carbon-H-bond
E268@O-CI@F4	3.19	-	Halogen	Halogen (Fluorine)
T301@HG21-CI	2.93	-	Hydrophobic	Pi-Sigma
CI-F283	4.36	-	Hydrophobic	Pi-Pi stacked
M304-CI	5.15	-	Hydrophobic	Amide-Pi stacked
V281-CI	5.14	-	Hydrophobic	Alkyl
CI@C2-L272	5.04	-	Hydrophobic	Alkyl
L272-CI	5.23	-	Hydrophobic	Pi-Alkyl
F283-CI@C2	3.73	-	Hydrophobic	Pi-Alkyl
F356-CI	4.51	-	Hydrophobic	Pi-Alkyl
L369-CI	4.56	-	Hydrophobic	Pi-Alkyl
CI-V281	5.03	-	Hydrophobic	Pi-Alkyl
CI-L299	5.23	-	Hydrophobic	Pi-Alkyl
CI-V235	5.22	-	Hydrophobic	Pi-Alkyl
CI-A248	4.12	-	Hydrophobic	Pi-Alkyl
CI-M304	5.39	-	Hydrophobic	Pi-Alkyl
WNK1-AI				
R255@HE-AI@O11	2.11	145.87	Hydrogen-bond	Conventional-H-bond
R255@HH21-AI@O11	2.23	147.72	Hydrogen-bond	Conventional-H-bond
R255@HH21-AI@O25	2.51	134.13	Hydrogen-bond	Conventional-H-bond
AI@H23-V281@O	2.07	144.17	Hydrogen-bond	Conventional-H-bond
AI@H243-V281@O	2.99	110.30	Hydrogen-bond	Carbon-H-bond
F265-AI	4.93	-	Hydrophobic	Pi-Pi T-shape
L369-AI	4.59	-	Hydrophobic	Amide-Pi stacked
R255-AI	5.25		Hydrophobic	Alkyl
A372-AI@Cl3	4.06	-	Hydrophobic	Alkyl
AI-L252	5.15	-	Hydrophobic	Alkyl
AI@Cl3-L272	5.36	-	Hydrophobic	Alkyl
AI@Cl3-I345	3.99	-	Hydrophobic	Alkyl
AI@Cl3-L369	4.27	-	Hydrophobic	Alkyl
F232-AI	5.43	-	Hydrophobic	Pi-Alkyl
AI-L299	4.81	-	Hydrophobic	Pi-Alkyl
AI-L369	5.46	-	Hydrophobic	Pi-Alkyl
AI-A269	5.37	-	Hydrophobic	Pi-Alkyl
AI-L369	4.47	-	Hydrophobic	Pi-Alkyl
AI-L272	5.29	-	Hydrophobic	Pi-Alkyl

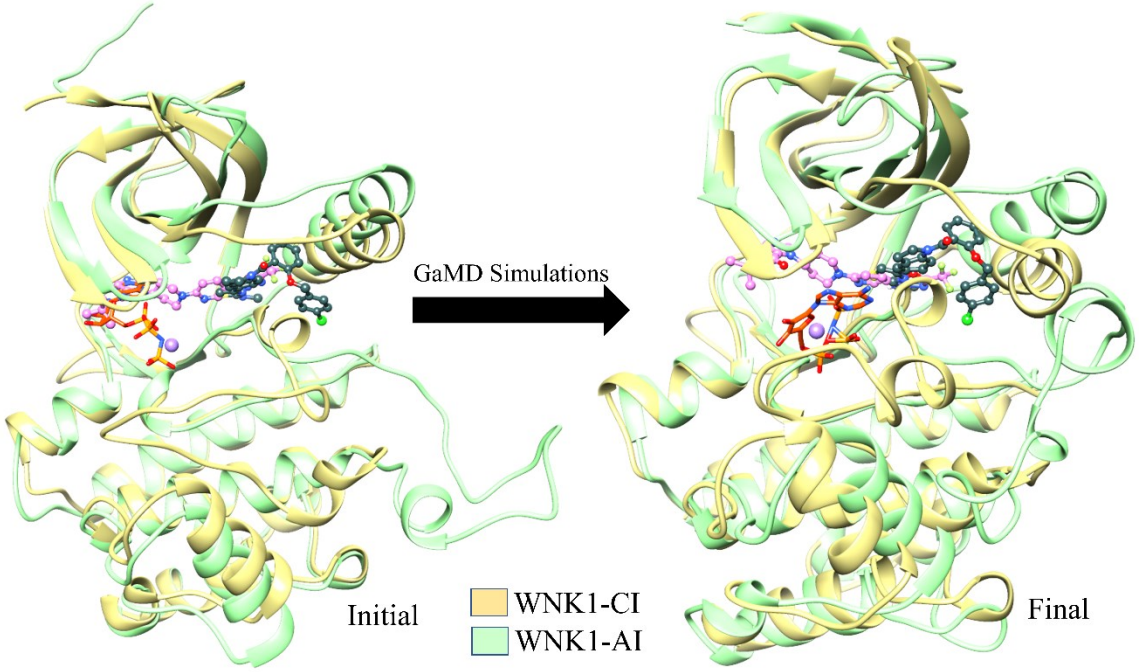

Figure S1. Superimposed structures of the WNK1-CI (PDB: 5DRB) and WNK1-AI (PDB: (5TF9) complexes before simulations (Initial) and the last trajectory structures of the complexes after GaMD simulations of 1 μs (Final).

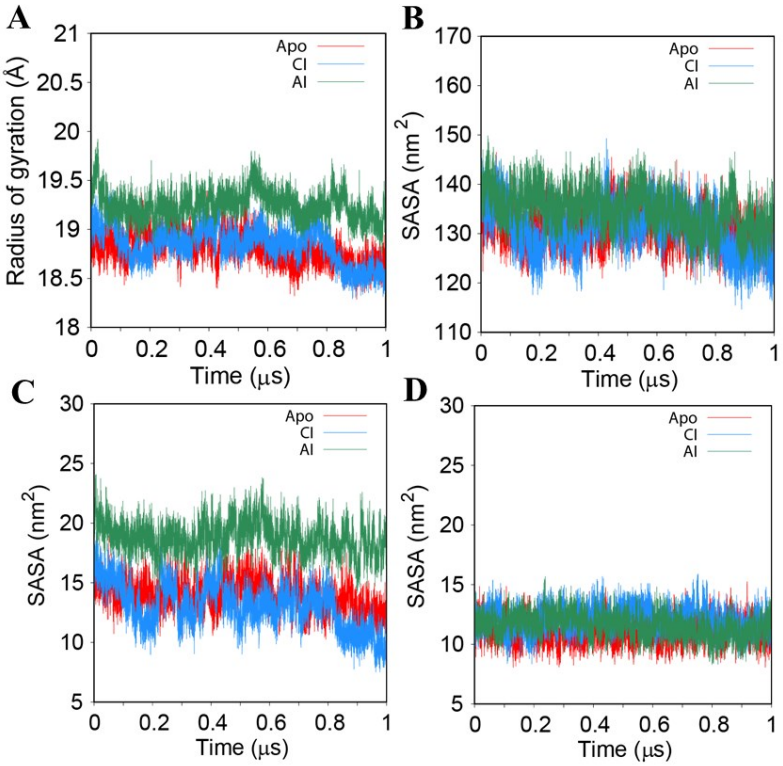

Figure S2. (A) Time evolution of the radius of gyration (R_g) of the *apo* (red), WNK1-CI (blue), and WNK1-AI (green) complexes (B), (C), and (D) Time evolution of the solvent-accessible surface area (SASA) for the whole, A-loop region, and αC-helix, respectively.

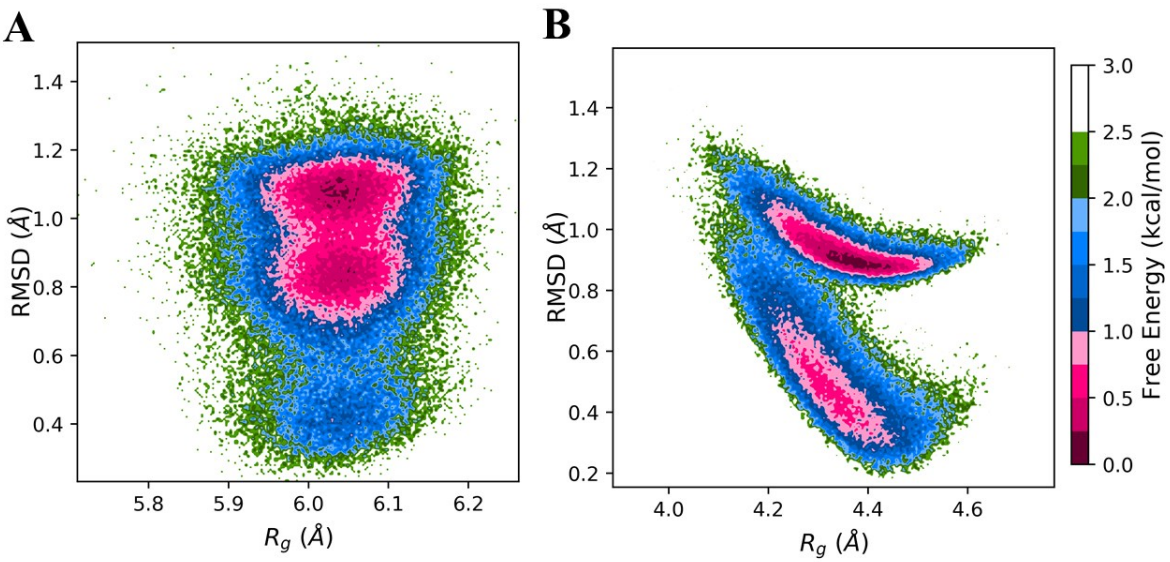

Figure S3. Free energy landscape of the WNK1-ligand complexes for R_g vs. RMSD of the ligand (A) WNK1-CI (B) WNK1-AI.

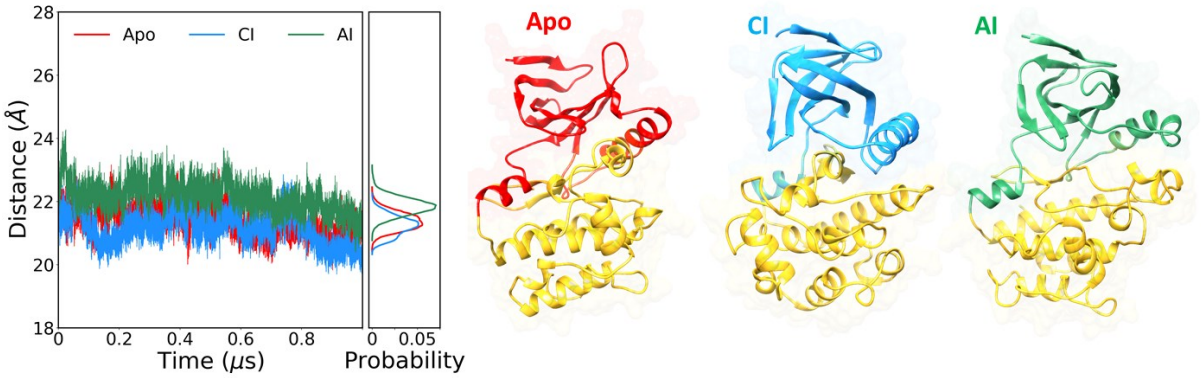

Figure S4. Time evolution of the distance between the N-lobe and C-lobe in Apo (maroon), WNK1-CI (blue), and WNK1-AI (green) complexes. Its cartoon representations are also shown for the systems from the last PDB structure.

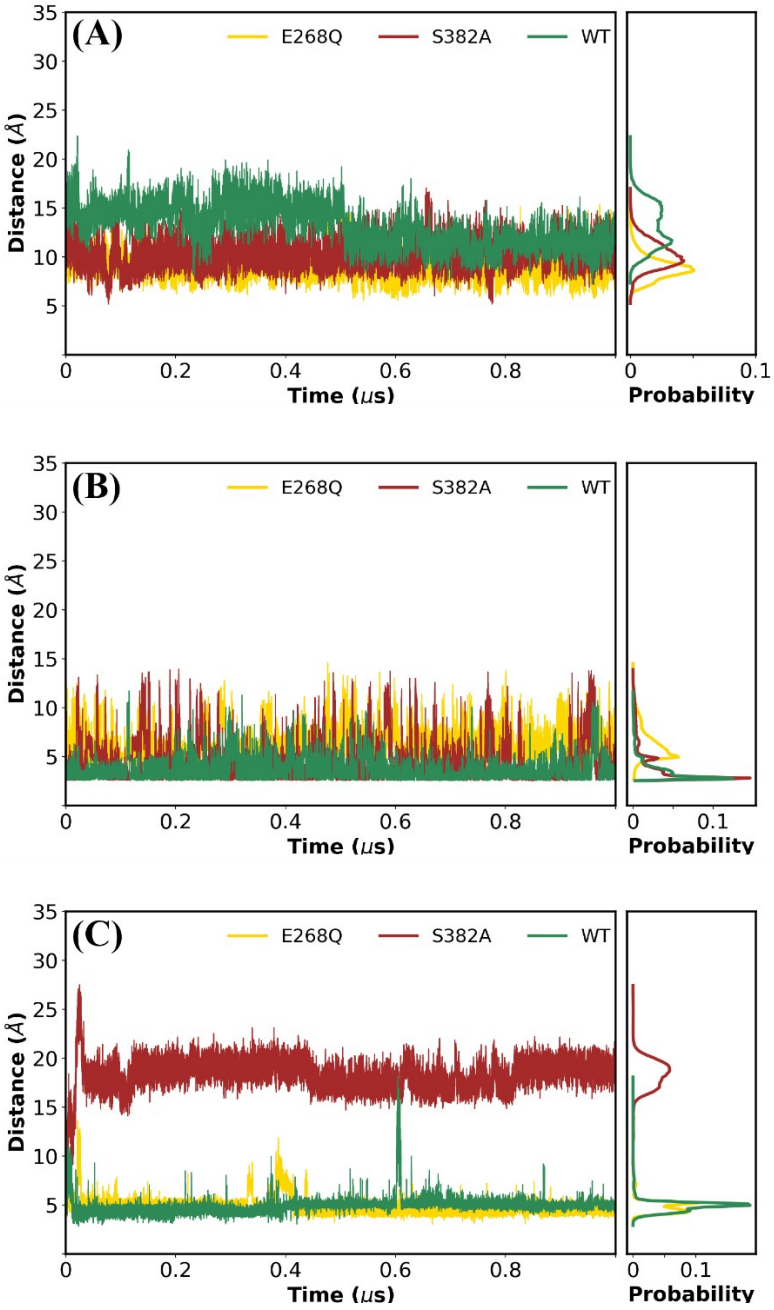

Figure S5. Interactions affecting the binding pocket in WNK1 upon binding of allosteric inhibitor in wild-type (WT) is compared with two mutations, namely E268Q and S382A, respectively. (A-C) showing the various interactions, including the salt-bridge between residues such as E268-R348, E268-R264, and S382-R348, respectively (interaction residues naming as per the WT).

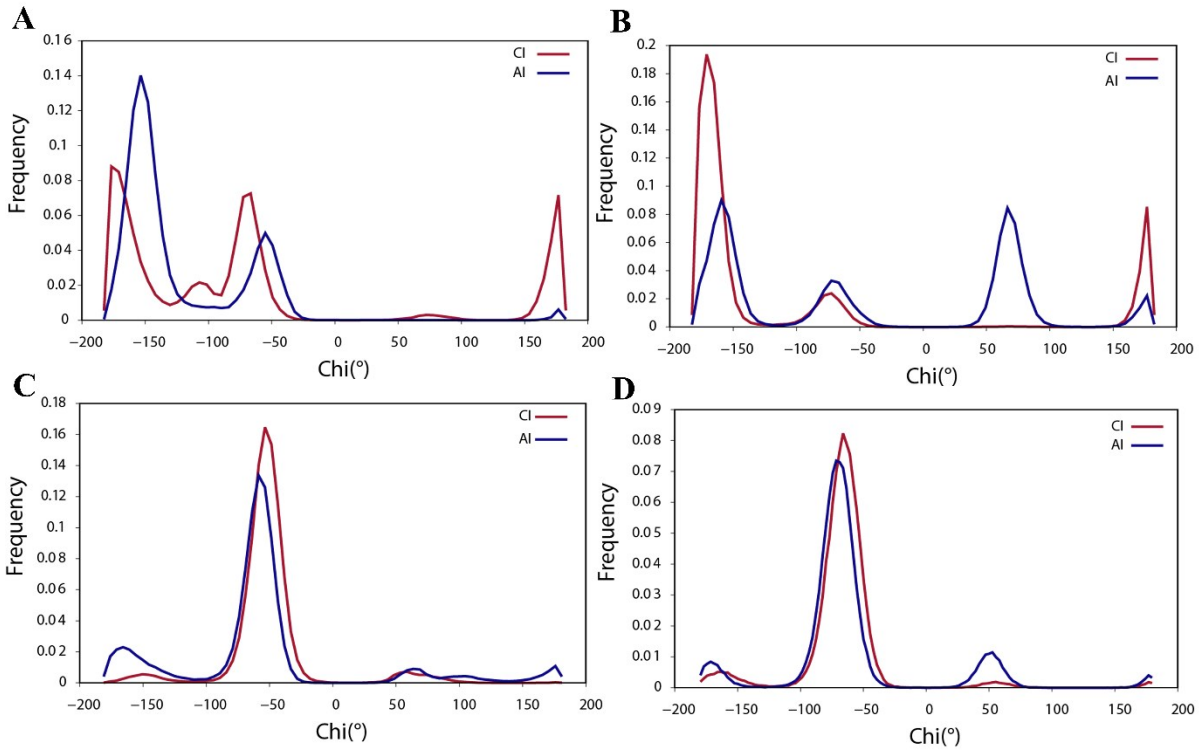

Figure S6. Frequency distribution of the dihedral angles (χ) χ_1 from GaMD trajectories for both complexes, WNK1-CI and WNK1-AI in (A) E268 (B) R264 (C) R348 (D) S382.

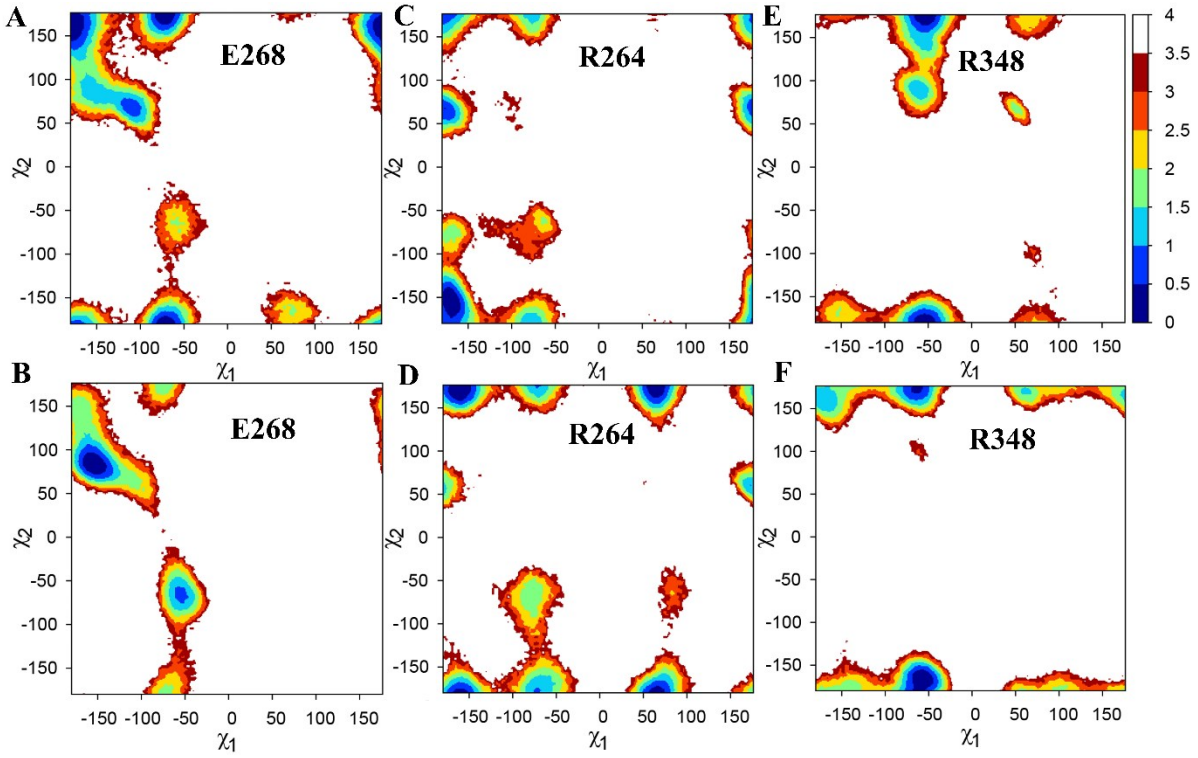

Figure S7. Contour maps of free energies as a function of side-chain dihedral angles (chi) χ_1 and χ_2 for residues E268, R264, and R348 of (A, C, E) WNK1-CI (B, D, F) WNK1-AI complex, respectively.

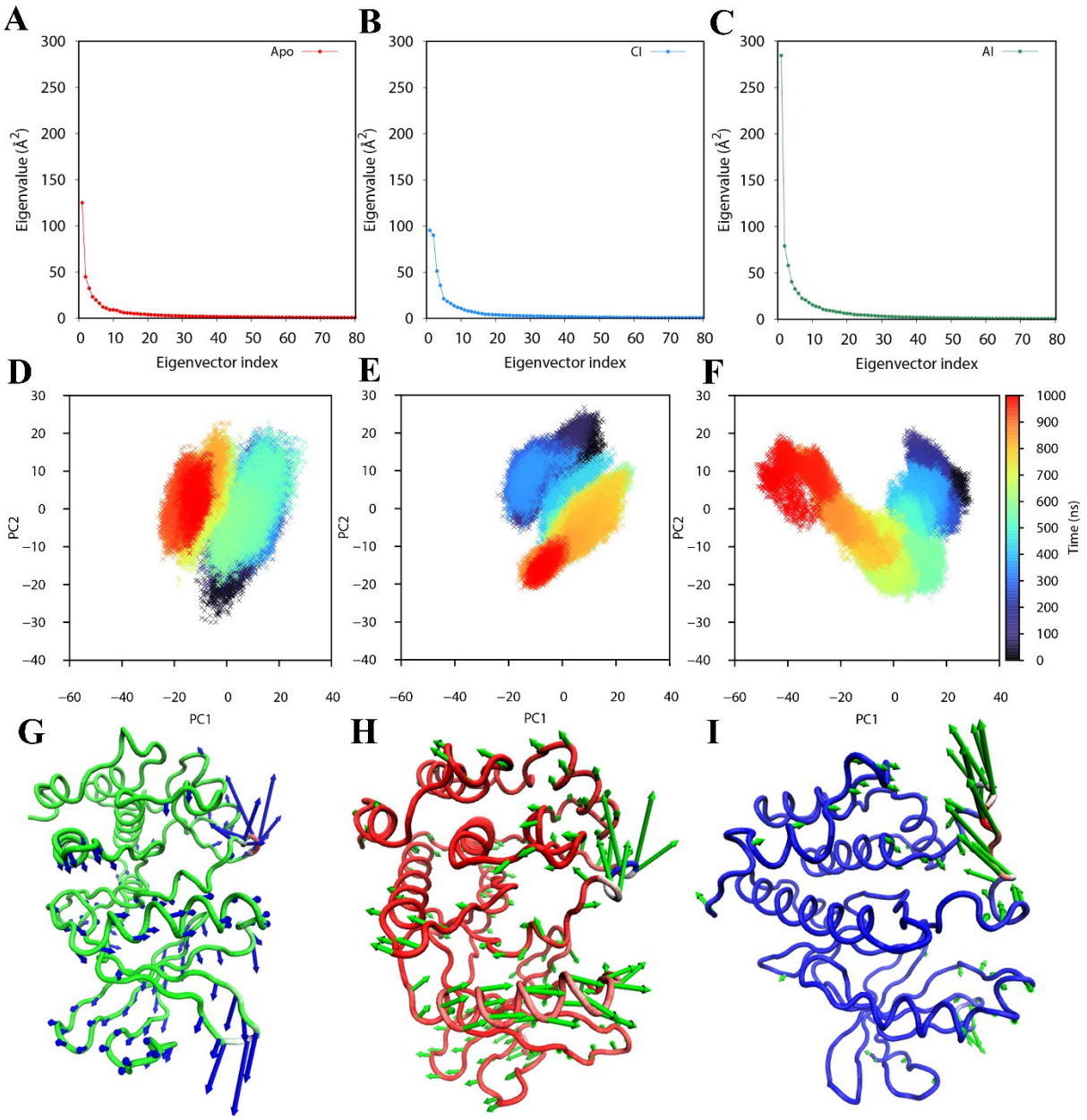

Figure S8. PC modes (eigenvectors) to the overall motions for (A) Apo (B) WNK1-CI (C) WNK1-AI. (D-F) 2D projection of PC1 and PC2 from GaMD trajectories with time. (G-I) showing the PCA porcupine plots for Apo, CI, and AI complex, respectively. The arrowhead shows the direction of motion, while length indicates the magnitude of the motions.

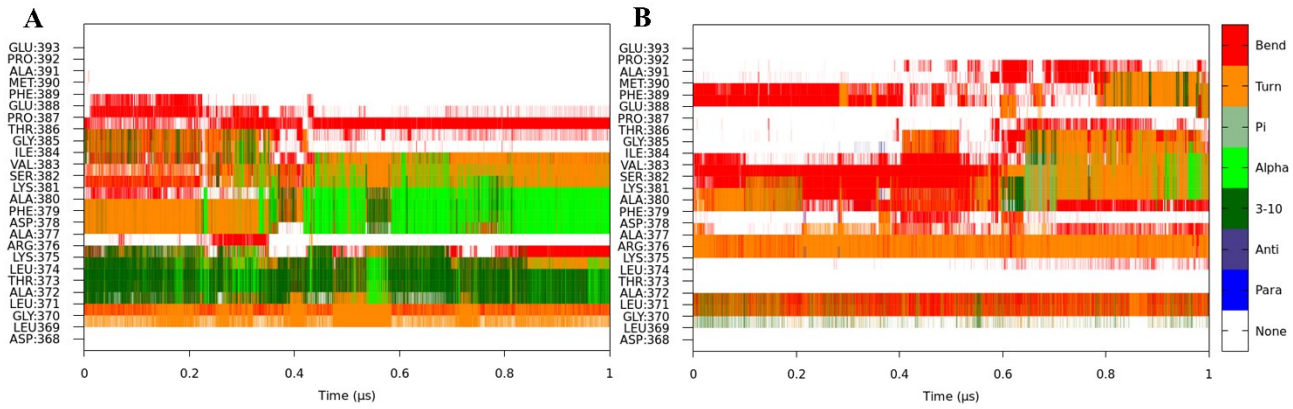

Figure S9. The secondary structure (DSSP) of the A-loop region from the GaMD simulations trajectories for (A) WNK1-CI and (B) WNK1-AI complex.

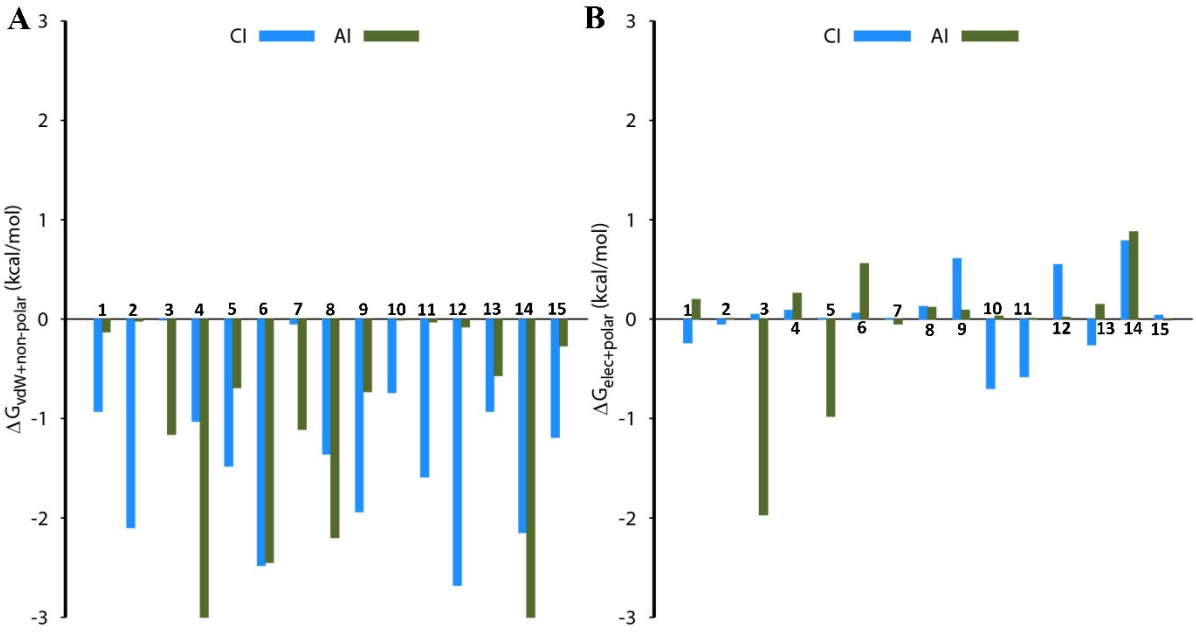

Figure S10. Comparison of the per-residue energy decomposition of the key residues involved in the binding of the WNK1-CI and WNK1-AI complexes (A) The sum of vdW and non-polar solvation energy, $\Delta E_{vdW,}$ ΔG_{np}. (B) The sum of electrostatic and polar solvation energy, $\Delta E_{elec\ +,}$ ΔG_{pol}. Key residues involved: **1**-K233, **2**-V235, **3**-R255, **4**-L272, **5**-V281, **6**-F283, **7**-I297, **8**-L299, **9**-T301, **10**-L303, **11**-M304, **12**-F356, **13**-G367, **14**-L369, **15**-L371.

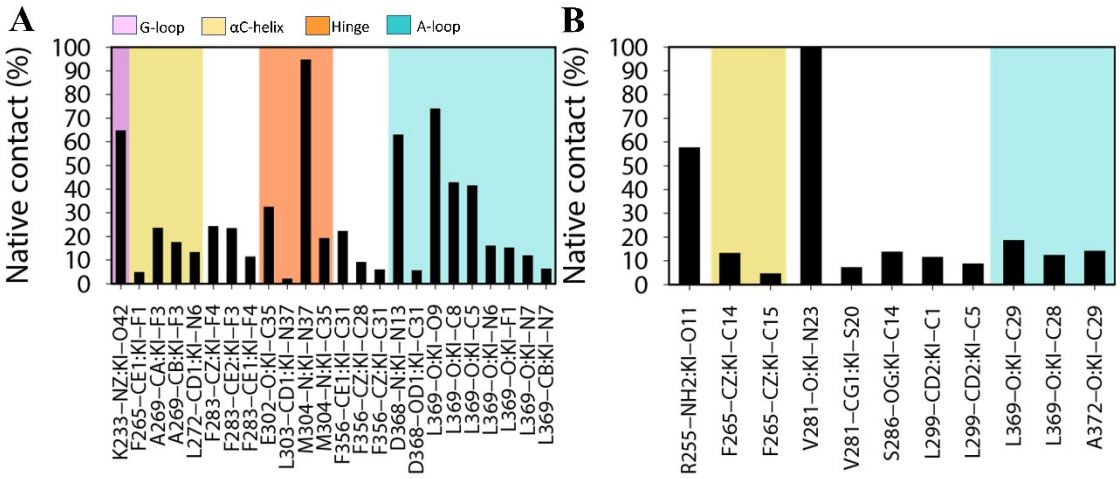

Figure S11. Percentage of native contact between WNK1-inhibitors. Significant regions such as G-loop, αC-helix, Hinge, and A-loop are highlighted in pink, yellow, orange, and cyan color, respectively. (A) WNK1-CI and (B) WNK1-AI complex.

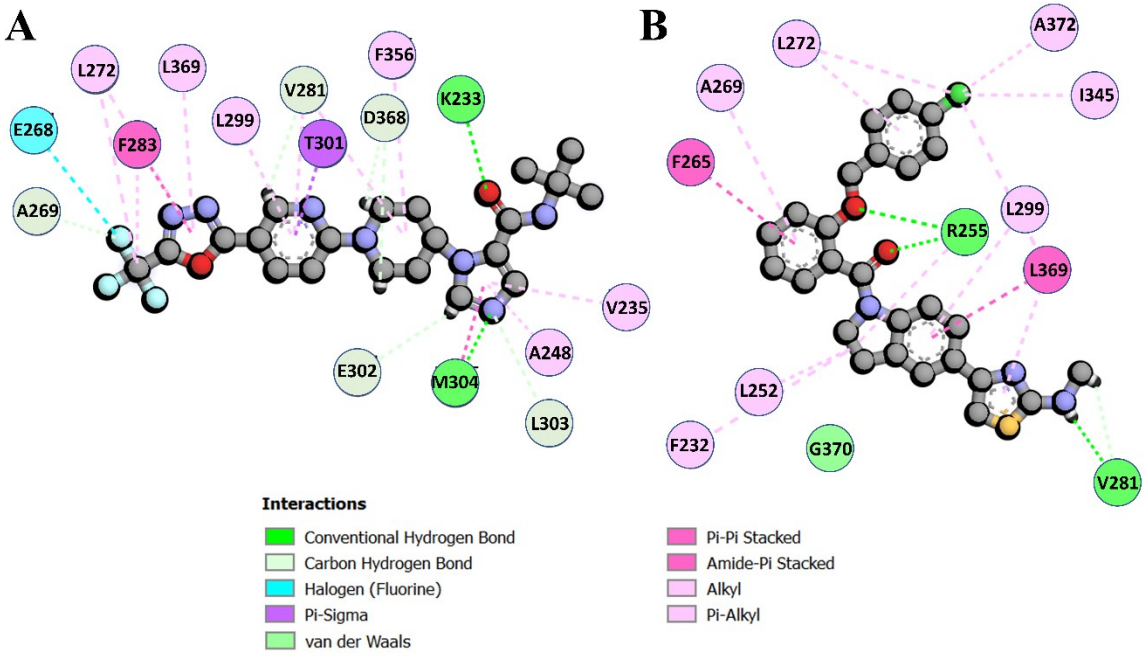

Figure S12. The non-bonded WNK1-inhibitors interactions calculated from the last trajectory of the GaMD simulations by using the Discovery studio for the complexes (A) WNK1-CI and (B) WNK1-AI.